ISBN: 978-3-95450-253-0 ISSN: 2673-5571 doi:10.18429/JACoW-HB2023-THC2C1

SHOWER SIMULATIONS FOR THE CERN PROTON SYNCHROTRON INTERNAL DUMP AND COMPARISON WITH BEAM LOSS MONITOR DATA

S. Niang*,[1], D. Domange[2], L. S. Esposito[1], M. Giovannozzi[1], C. Hernalsteens[1], A. Huschauer[1], T. Pugnat[1]
[1]CERN, Geneva, Switzerland
[2]Université libre de Bruxelles, Brussels, Belgium

Abstract

During the Long Shutdown 2 (LS2), two new internal dumps (TDIs) were installed and successfully put into operation in the CERN Proton Synchrotron (PS) to withstand the intense and bright beams produced for the High Luminosity LHC. TDIs serve as safety devices designed to rapidly enter the beam trajectory and stop the beam over multiple turns. Due to their design, the TDI only absorbs a fraction of the secondary particle shower produced by beam particles that impinge on it. Starting from impacts computed by multi-turn beam dynamics simulations, detailed shower simulations were performed with FLUKA to assess the radiation field's impact on the downstream equipment, with a particular emphasis on the dose measured by Beam Loss Monitors. The numerical data obtained from the simulations are compared with the experimental data collected during PS operation.

INTRODUCTION

The internal dumps of the PS ring, located in straight sections (SS) 47 and 48 of the accelerator, underwent a complete redesign to be installed during LS2 from 2019 to 2021. This was to make the internal dumps compatible with the increase in beam brightness as a result of the implementation of the LHC Injector Upgrade (LIU) project [1, 2]. Extensive studies were carried out to validate the thermomechanical limits of the new dump design [3, 4] and its efficiency in stopping the beams produced in PS after LS2 [5]. In the study [6], a standalone dump simulation was implemented in FLUKA [7, 8], along with a 5-dimensional matrix to transport beam particles throughout the rest of the accelerator. This matrix described the multi-passage of the beam particles by the dump location. Additionally, the movement of the dump was included during the revolution time.

In this study, our primary objective is to identify any energy deposition hot spots when utilising the dumps, and, if necessary, enhancing the shielding in these locations will be considered.

NUMERICAL SIMULATIONS

A significant difference from previous studies is the implementation in FLUKA of an extended and detailed model of the PS ring over the sections where the particle showers are absorbed. This required the input of the distribution of primary particles at the dump location obtained from a beam dynamic code, SixTrack [9, 10], in our case, coupled with FLUKA to describe in detail the mechanical aperture along the PS ring, while accurately accounting for the beam-matter interactions occurring in the moving internal dump [11] and the beam dynamics in the rest of the ring. The results of these simulations provide the position, direction, and energy of primary protons when they impact the dump at each turn. This distribution is loaded as source term into the FLUKA simulation, taking into account the dump's position at each turn. The tracking of the shower particles starts from SS47 and ends at SS69. Figure 1 shows a 3D visualisation of the geometry model. It should be noted that due to the dump speed of approximately 0.8 m s^{-1}, the beam is fully stopped after about a thousand turns, which corresponds to about a few ms in duration[1].

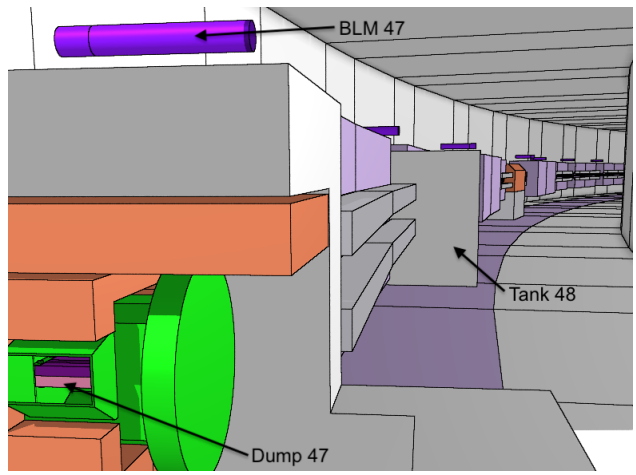

Figure 1: 3D visualisation of the PS ring FLUKA model using FLAIR [12].

We have considered three different operational scenarios:

- Activation of TDI.47 with the LHC beam at flat top, with a momentum of $p = 26.4\,\mathrm{GeV}/c$.
- Activation of TDI.48 with the same LHC beam.
- Activation of TDI.47 with the beam for the fixed-target programme at CERN's Super Proton Synchrotron (SPS) ring (SFTPRO), with a momentum of $p = 14.0\,\mathrm{GeV}/c$.

* samuel.niang@cern.ch

[1] Note that the revolution time is approximately 2.1 µs.

ISBN: 978-3-95450-253-0 ISSN: 2673-5571 doi:10.18429/JACoW-HB2023-THC2C1

COMPARISON WITH THE LOSS MAPS

The simulation predictions have been verified by benchmarking with the dose measured by the Beam Loss Monitors (BLMs) installed in the PS ring [13]. During dedicated Machine Development studies, the dumps were deliberately activated at various beam intensities to determine the dose recorded in each BLM per stopped beam primary particle.

From the NXCALS database [14], extensive arrays of parameters associated with accelerator operation can be extracted. Figure 2 displays the time evolution of the charge, momentum, and dose in the BLM.47 throughout a typical LHC accelerator cycle. By identifying the time of dump activation, the dose measured by each BLM can be determined. In the results, the statistical uncertainty is derived by 5 to 10 measurements at various beam intensity. The systematic uncertainty arising from the response of the BLMs and of the beam current transformer will be evaluated in a subsequent version of this study.

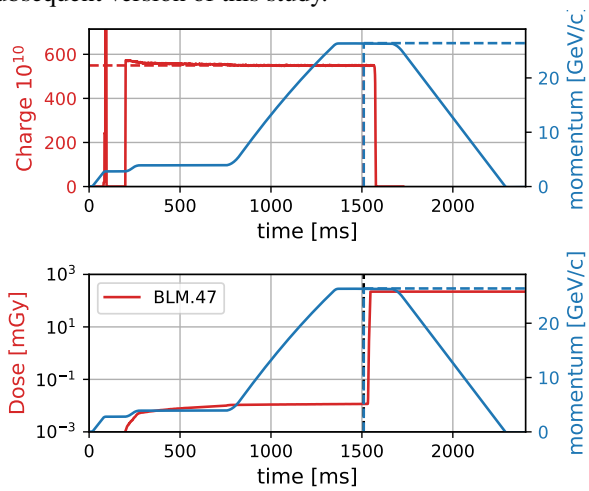

Figure 2: The blue curves show the momentum throughout a typical LHC cycle. Top: The red curve represents the beam intensity evolution. Bottom: The red plot shows the cumulative dose recorded by BLM.47. Dashed lines indicate the time when the TDI.47 is activated.

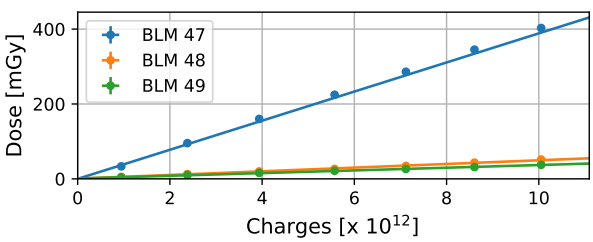

Figure 3: Dose recorded in the three first BLMs for the case of the LHC beam at flat-top when the TDI.47 is activated.

As illustrated in Fig. 2, the beam intensity stopped by the dump is determined as the charge measured at a time immediately before the dump activation. The dose is calculated as the accumulated dose measured by the BLM, opportunely excluding losses occurring before the activation of the dump. A linear response of these detectors is observed (Fig. 3) as a function of the beam intensity.

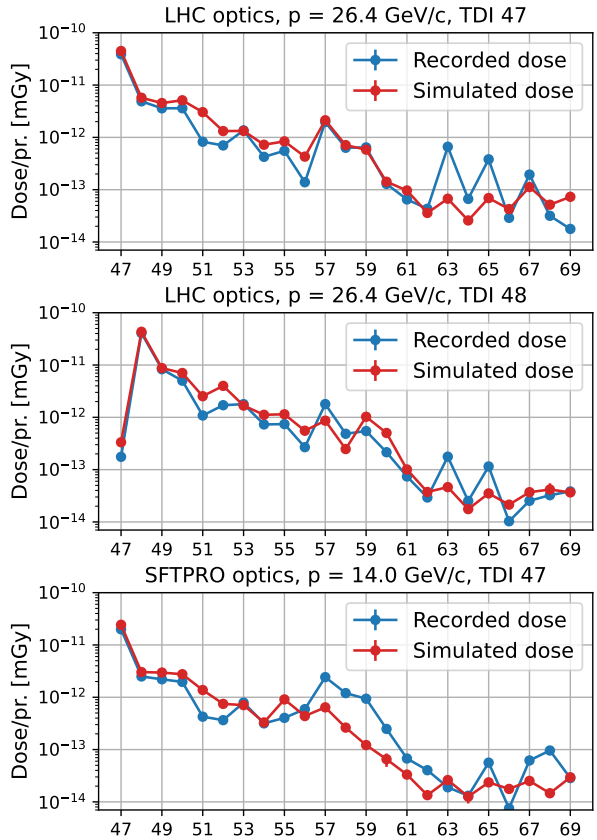

Figure 4: Loss maps measured by the BLMs (blue) and computed from the FLUKA simulation (red). Top): LHC case at flat-top when the TDI.47 is activated. Middle: LHC case at flat-top when the TDI.48 is activated. Bottom: SFTPRO case at flat-top when the TDI.47 is activated.

The comparison of the simulation results with the measured data is shown in Fig. 4. Overall, there is good agreement in the patterns, spanning almost four orders of magnitude. However, a discrepancy is observed in the correspondence of the extraction region, SS62–SS65, in particular with the LHC beam when TDI.47 is activated. Regarding the SFTPRO beam, the simulation underestimates the dose measured in SS57–SS62. Those observations suggest the need for further investigations in the aperture model and in the closed-orbit offset, which were not included in the simulations. Closed orbits have been measured each time the dumps were activated, as shown in Fig. 5. For the LHC beam case, the measured offset can be as large as 1 cm in the horizontal plane and about 5 mm vertically. Furthermore, a sensitivity study with respect to the position of BLMs will be included in future analyses.

RESULTS

Figure 6 illustrates the energy density absorbed by the TDI.47 for an LHC beam at flat top. Following the specification in Ref. [15], the assumed number of stopped protons is 5×10^{13}, which represents the most conservative scenario. For each pulse, the energy deposited in the dump amounts to

ISBN: 978-3-95450-253-0 ISSN: 2673-5571 doi:10.18429/JACoW-HB2023-THC2C1

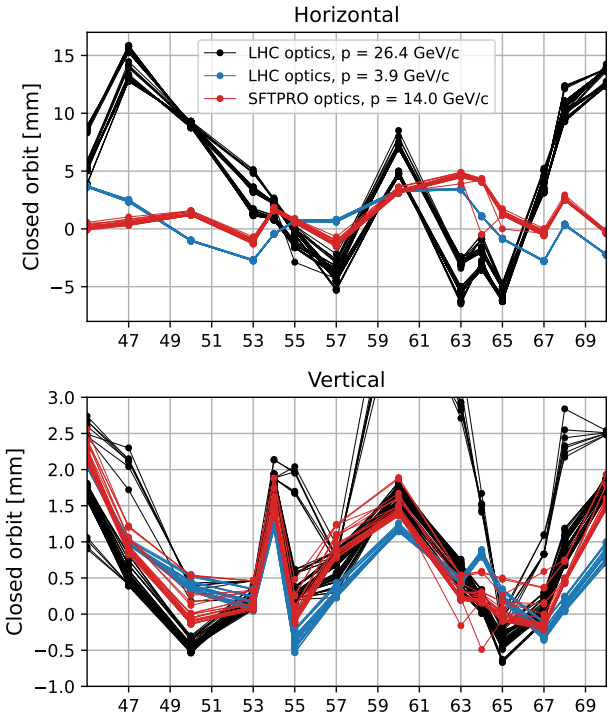

Figure 5: Closed orbits measurements for different beams and energies in SS47–SS69. Top: horizontal closed orbit. Bottom: vertical closed orbit.

8.4 kJ, which constitutes 6.5% of the available beam kinetic energy. This is consistent with the findings in Ref. [4].

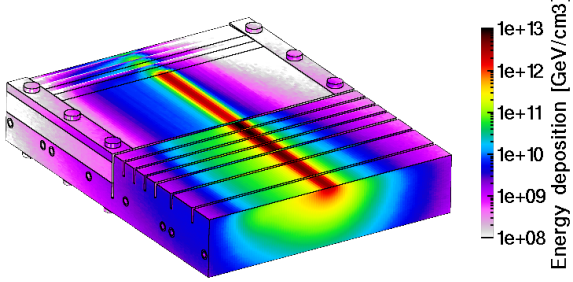

Figure 6: Energy density in the TDI.47 when it is activated to stop a LHC beam at flat-top ($p = 26.4\,\mathrm{GeV}/c$) normalised to an intensity of 5×10^{13} protons.

Table 1 provides information on the locations where the remaining energy is absorbed. It can be seen that nearly 50% of the total kinetic energy of the beam is absorbed by the main magnets, while the tank and the shielding surrounding the dump absorb 14.1% of the energy. A fraction escapes the region primarily in the form of neutrinos, whereas another fraction is converted to mass in nuclear reactions.

In Fig. 7, the accumulated yearly dose is shown in both the main magnets and in the BLMs. As indicated in Ref. [15], it was assumed that the dump stops 2.4×10^{17} protons. Conservatively, we have considered that all protons are stopped in conditions of the LHC case at flat top. The magnets in the first three sectors downstream of the dump experience the highest exposure, with an absorbed dose at least a factor of

Table 1: Breakdown of the absorbed energies in the different equipment and in the tunnel wall for a LHC beam at flat-top ($p = 26.4\,\mathrm{GeV}/c$) when the TDI.47 is activated.

Absorption mechanism	**% of the beam kinetic energy**
Main magnets	49.8
Tank/shielding TDI.47	14.1
Tunnel wall	11.3
TDI.47	6.5
Tank/shielding TDI.48	4.8
Other elements	3.5
Beam pipes	2.4
Air	0.1
Mass production from nuclear reactions	6.3
Neutrinos	1.2

10 higher than those farther downstream. Moreover, the dose absorbed by the coils is an order of magnitude greater than that of the yoke. This highlights potential localised energy deposition hot-spots, which will be further investigated.

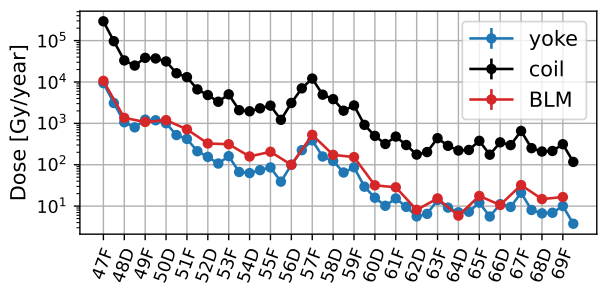

Figure 7: Total integrated dose in the yoke and coils of main magnets accumulated after a year operation (2.4×10^{17} protons per year) for a LHC beam at flat-top ($p = 26.4\,\mathrm{GeV}/c$) when the TDI.47 is used. The absorbed dose in BLMs is also shown.

CONCLUSION AND OUTLOOK

This study has established good agreement between the simulated results and the measurements when the PS internal dumps are operated. With approximately 7% of the beam energy absorbed by the dump, the remaining energy is predominantly absorbed by the beam line elements and the surrounding walls. In a follow-up of this study, the analysis and comparison with data will be further refined, including a more thorough evaluation of the systematic errors associated with both the dose and charge intensity measurements. Additionally, a sensitivity study due to the positioning of the BLMs and the implementation of the closed orbit in the simulations will also be addressed. Considering the appropriate sharing between the different beams, the model prediction will be used to assess the absorbed dose in the sensitive equipment and, if necessary, implement additional protective shielding measures.

ISBN: 978-3-95450-253-0 ISSN: 2673-5571 doi:10.18429/JACoW-HB2023-THC2C1

REFERENCES

[1] H. Damerau *et al.*, *LHC Injectors Upgrade, technical design report*. CERN, 2014. doi:10.17181/CERN.7NHR.6HGC

[2] *LHC Injector Upgrade Project*, https://espace.cern.ch/liu-project/default.aspx.

[3] G. Romagnoli *et al.*, "Design of the new PS internal dumps, in the framework of the LHC Injector Upgrade (LIU) Project," in *Proc. IPAC'17*, Copenhagen, Denmark, May 2017, pp. 3521–3523. doi:10.18429/JACoW-IPAC2017-WEPVA109

[4] G. Romagnoli *et al.*, "Engineering design and prototyping of the new LIU PS internal beam dumps," in *Proc. IPAC'18*, Vancouver, Canada, Apr.-May 2018, pp. 2600–2603. doi:10.18429/JACoW-IPAC2018-WEPMG001

[5] R. Steerenberg and D. Cotte, "PS beam spot sizes for the design of new internal beam dumps," CERN, Tech. Rep., 2017. https://edms.cern.ch/ui/file/1612293/1/PS_Beam_Size_Calculations_InternalDumps.pdf

[6] J. A. B. Monago *et al.*, "Multi-turn study in FLUKA for the design of CERN-PS internal beam dumps," in *Proc. IPAC'18*, Vancouver, Canada, Apr.-May 2018, pp. 724–727. doi:10.18429/JACoW-IPAC2018-TUPAF025

[7] G. Battistoni *et al.*, "Overview of the FLUKA code," *Ann. Nucl. Energy*, vol. 82, pp. 10–18, 2015. doi:10.1016/j.anucene.2014.11.007

[8] C. Ahdida *et al.*, "New capabilities of the FLUKA multi-purpose code," *Front. Phys.*, vol. 9, 2022. doi:10.3389/fphy.2021.788253

[9] R. De Maria *et al.*, SixTrack – *6D tracking code*, http://sixtrack.web.cern.ch/SixTrack/.

[10] R. D. Maria *et al.*, "SixTrack version 5: status and new developments," in *Proc. IPAC'19*, Melbourne, Australia, May 2019, pp. 3200–3203. doi:10.18429/JACoW-IPAC2019-WEPTS043

[11] T. Pugnat *et al.*, "Study of the performance of the CERN Proton Synchrotron internal dump," presented at HB'23, Geneva, Switzerland, Oct. 2023, paper THBP36.

[12] V. Vlachoudis, "FLAIR: A powerful but user friendly graphical interface for FLUKA," in *Proc. Int. Conf. on Mathematics, Computational Methods & Reactor Physics (M&C 2009)*, 2009. https://cds.cern.ch/record/2749540

[13] S. S. Gilardoni *et al.*, "Beam loss monitors comparison at the CERN Proton Synchrotron," Tech. Rep., 2011. https://cds.cern.ch/record/1382024

[14] J. Wozniak and C. Roderick, "NXCALS - Architecture and challenges of the next CERN accelerator logging service," in *Proc. ICALEPCS'19*, New York, NY, USA, 2020, pp. 1465–1469. doi:10.18429/JACoW-ICALEPCS2019-WEPHA163

[15] F.-X. Nuiry and G. Romagnoli, "PS ring internal dumps functional specifications," CERN, Tech. Rep., 2017. https://edms.cern.ch/ui/file/1582110/2.1/PS-TDI-ES-0001-20-10.pdf